Lessons Learned during the Integration Phase of the NASA IN-STEP Cryo System Experiment

R. S. Sugimura

Jet Propulsion Laboratory
California Institute of Technology
Pasadena, CA 91109 USA

S. C. Russo and D. C. Gilman

Hughes Aircraft Company
Electro Optical Systems
El Segundo, CA 90245 USA

ABSTRACT

The Cryo System Experiment (CSE), a NASA In-Space Technology Experiments Program (IN-STEP) Class D Flight Experiment, was developed by Hughes Aircraft Company to validate in zero-g space a 65 K cryogenic system for focal planes, optics, instruments, or other equipment (gamma-ray spectrometers and infrared and submillimeter imaging instruments) that require continuous cryogenic cooling. The system consists of a long-life, low-vibration Stirling-cycle, 65 K, Improved Standard Spacecraft Cryocooler (ISSC), and a diode oxygen heat pipe thermal switch that enables physical separation between the cooling source and the element to be cooled.

A key value of this flight experiment has been the opportunity for Hughes and the Jet Propulsion Laboratory (JPL) to identify and resolve cooler and imaging-instrumentation integration issues that will be encountered when these enabling thermal management technologies are integrated in future space cryogenic cooling systems.

Presented are generic lessons learned from the system integration of cryocoolers for a flight experiment including: launch-vibration restraints for the expander cold-tips, implementation of compressor and expander hysteresis test capability, the design and installation of a high-compliance thermal strap to minimize side loads on the expander, the inclusion of both the cooler as well as its heat rejection materials in the mass calculation, contamination/parasitics, system operations/software, electrical interface requirements, and the safety implications associated with the classification of mechanical components and the radiation environment.

In *Cryocoolers 8*, Plenum Publishing Corp., New York, 1995, pp. 869-882.

The CSE is funded by the NASA Office of Advanced Concepts and Technology's IN-STEP and managed by JPL. Hughes conceived the experiment and completed the equivalent Phase A activity outside of IN-STEP through both government funded and internal research and development programs. The CSE Project has completed Phase B (mechanical, thermal and electrical design activities), Phase C/D (fabricate, assemble, test, and deliver the CSE to Goddard Space Flight Center), and will support the pre-flight, flight and post-flight data analysis activities for Flight 1 of this two-flight experiment. The CSE is currently at the Goddard Space Flight Center (GSFC) awaiting integration onto a Hitchhiker cross-bay carrier.

The overall goal of the CSE is to validate and characterize the on-orbit performance of three thermal management technologies that comprise a hybrid cryogenic system. These thermal management technologies consist of: 1) a second-generation long-life, low-vibration, Stirling-cycle, 65 K cryocooler that will be used to charge a thermal energy storage device (TRP), 2) a diode oxygen heat pipe thermal switch that enables physical separation between a cryogenic refrigerator and TRP, and 3) a nitrogen, triple-point thermal energy storage device to provide a stable cryogenic temperature source. This experiment is necessary to provide a high confidence zero-g database for the future design of cryogenic systems for multi-year space flight applications. The level of confidence that will be provided by this experiment is an important NASA and DoD requirement prior to multi-year mission commitment. The CSE illustrates an important type of NASA space-flight experiment in which an emerging technology is validated to provide the option for subsequent application in near-future space system developments.

The CSE was originally proposed as two separate flights. The first flight, the basis for this paper, includes the ISSC cryocooler and the diode oxygen heat pipe; it utilizes an aluminum sphere to simulate the nitrogen triple-point thermal energy storage device that is anticipated to be included in the second flight.

INTRODUCTION

In this experiment two types of coolers are used. The first is a Stirling-cycle, Hughes long-life, low-vibration, 65 K, 2 W, ISSC suitable for multi-year space missions. The technology benefits are significant to a number of science instruments selected for NASA's Earth Observing System (Eos) instruments and a number of space reconnaissance instruments. The unit consists of a compressor connected to an expander by a transfer tube, shown in Fig. 1, and the control electronics.

The second type of cryocooler is a rotary drive, tactical piston-driven Stirling cooler. This tactical cooler, shown in Fig. 2, has been designed by Hughes to have a relatively large cooling capacity and an anticipated life on the order of 1000 hours. This cooler has successfully flown on previous shuttle flight experiments to support a rapid cooldown to cryogenic temperatures allowing more time for the actual experiment to be performed at cryogenic temperature. Its predecessors have been used to cool sensors in aircraft and missiles where mechanical robustness and insensitivity to vibration are key requirements.

Figure 3 is a block diagram of the CSE with the ISSC connected to the simulated TRP mass through a thermal heat strap. One tactical cooler is connected through the diode oxygen heat pipe to the opposite side of the simulated TRP. This physical arrangement was selected to reduce risk should a failure occur within the heat pipe or the ISSC. In an operational system the diode oxygen heat pipe would be located between the ISSC and the thermal energy storage device. A second tactical cooler is used to minimize parasitics by cooling a radiation shield to

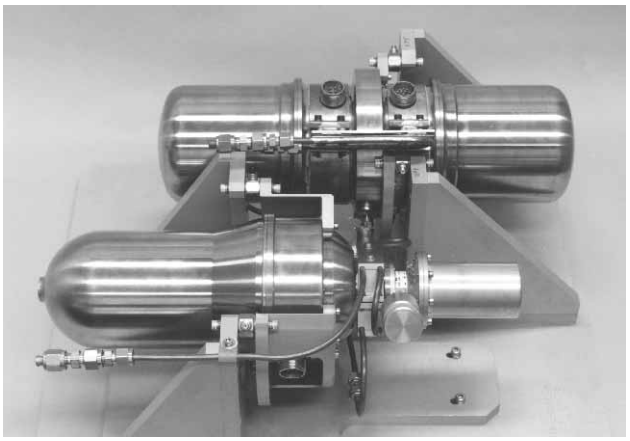

Figure 1. Hughes long-life, low-vibration, 65 K, 2 W, Improved Standard Spacecraft Cryocooler (ISSC).

Figure 2. Hughes Model 7044 H tactical cryocooler.

a temperature of approximately 120 K. In a non-shuttle flight system, shield cooling is generally provided by a cryogenic radiator.

Figure 4 shows the CSE mechanical assembly attached to the upper end plate (UEP). The ISSC and two tactical coolers are heat sunk to the UEP that acts as a radiator. The remainder of the experiment is connected to bipods through support and ballast rings that support the radiation shield and simulated TRP, and the canister electronics box, which contains sensor signal conditioning circuitry. The entire mechanical assembly is attached to, or suspended from, the UEP and secured in a 5 ft^3 canister. The canister and two electronics boxes are mounted on a cross-bay Hitchhiker carrier assembly with several other experiments, as shown in Fig. 5.

An important thrust of the CSE is the integration of the cryocoolers into this cryogenic system. Not only must the cryocoolers provide the necessary cooling capacity, they must also be thermally, mechanically, physically and electrically compatible with the rest of the instrument. As long-life, low-vibration cryocoolers transition from an emerging to an enabling technology, the focus shifts from cooler performance issues (volume, mass, thermal, input/output power, electrical) to system compatibility and integration issues. The following sections summarize the lessons learned during the system integration phase of this shuttle-flight experiment.

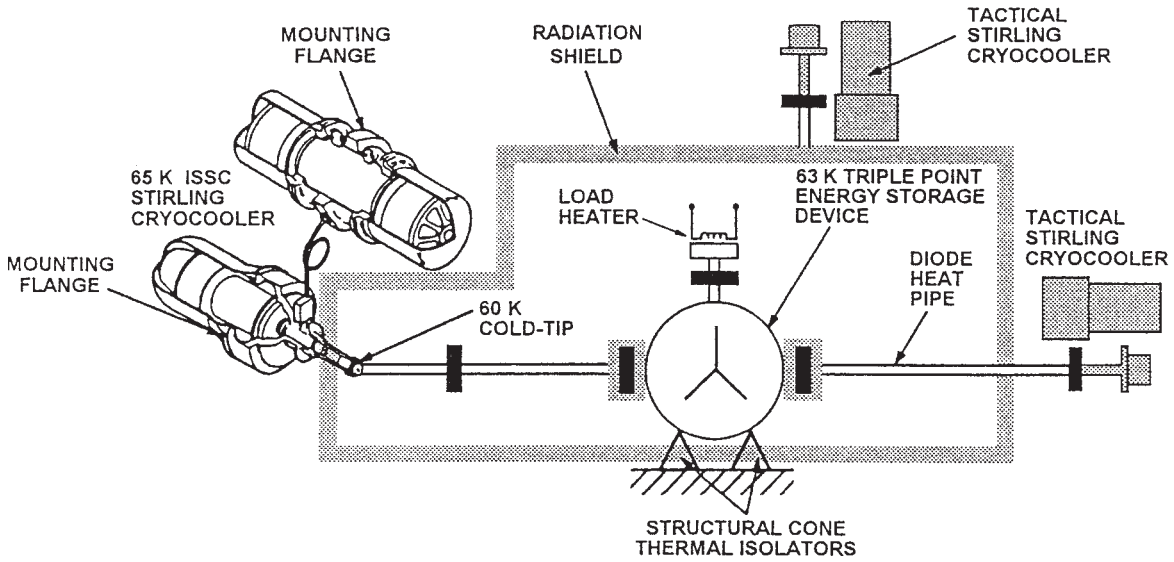

Figure 3. Cryo System Experiment block diagram.

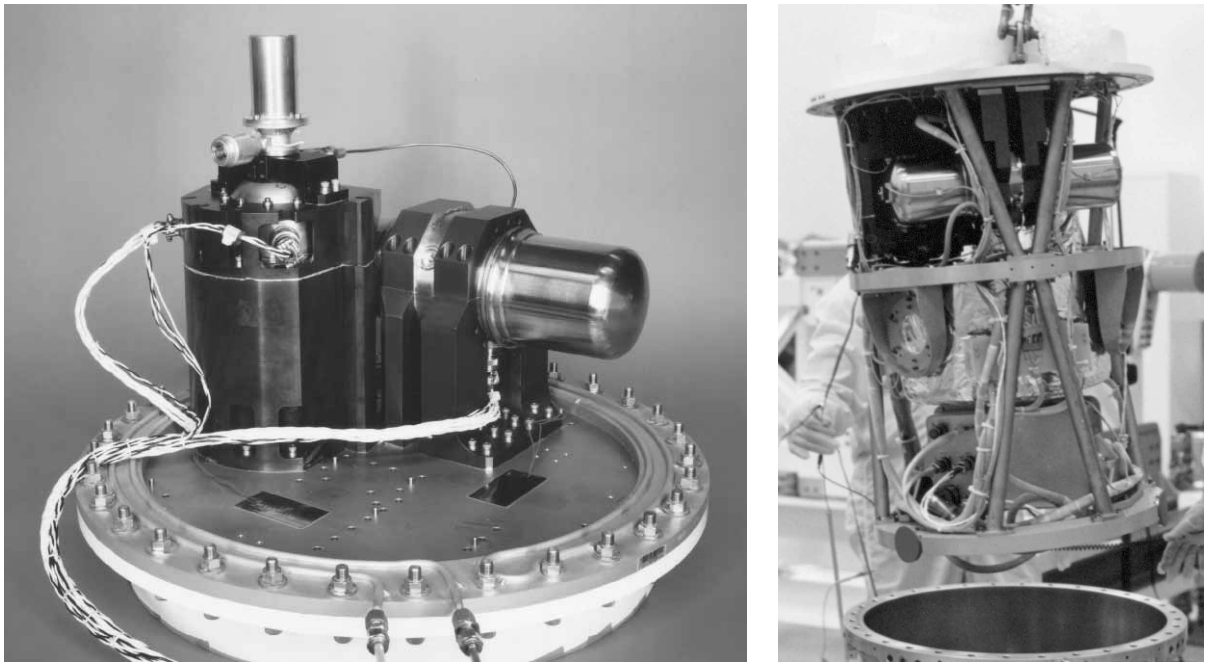

Figure 4. The CSE mechanical assembly attached to the upper plate.

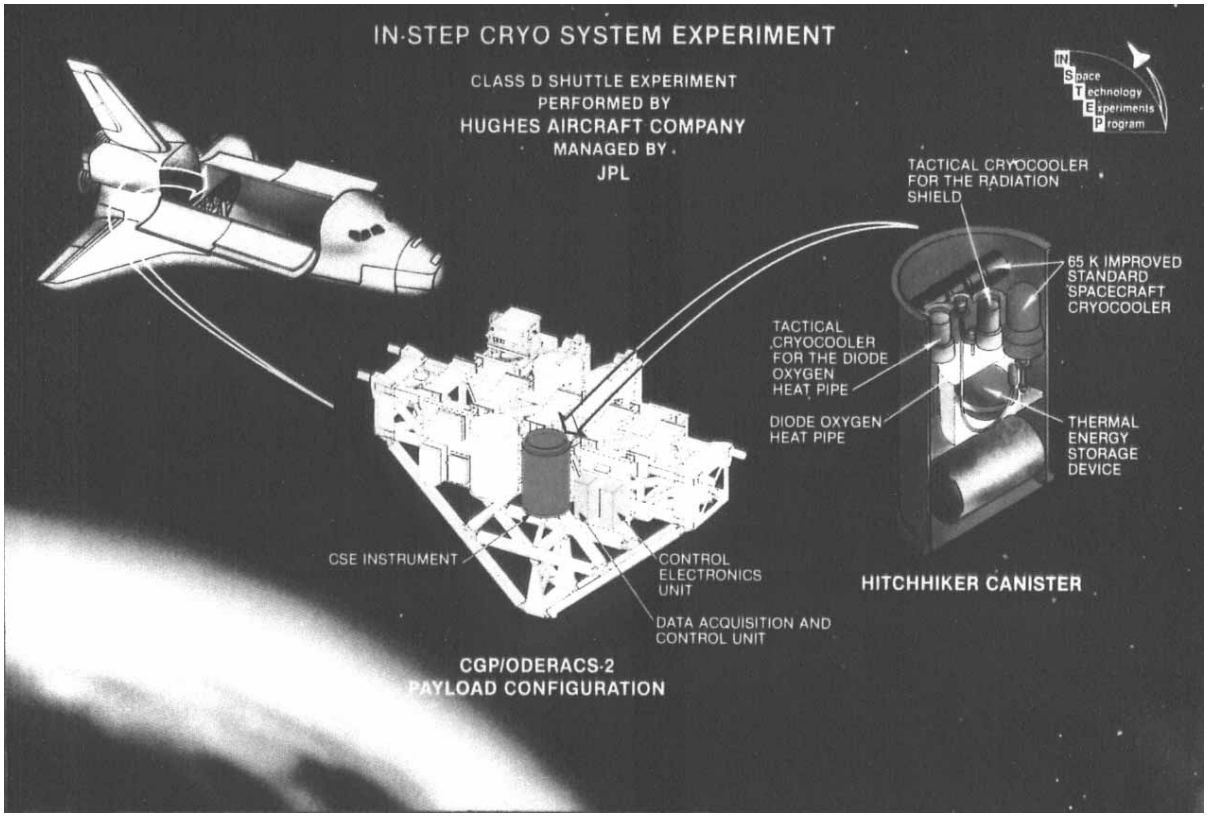

Figure 5. Cryo System Experiment mounted on a Hitchhiker cross-bay carrier within the obiter.

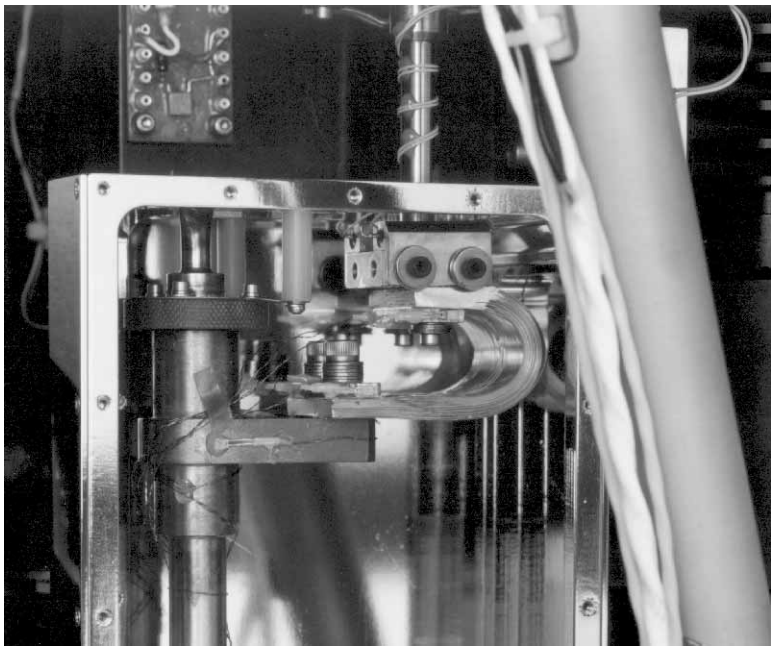

Figure 6. Heat pipe tactical cooler expander, interface mass, and thermal strap.

LAUNCH VIBRATION

A key challenge was to resolve the issue of launch vibration and the impact to the cryocooler expanders. The expander cold finger, a relatively thin-wall, hollow tube in which the expander piston shuttles, is necessarily thin to minimize parasitic thermal loads due to axial heat transfer. Although by itself the expander cold finger may be considered relatively robust, it is necessary to include a thermal transfer path to provide cooling to the load. This is accomplished by an interface between the expander cold-tip (usually a copper block) and a flexible thermal strap to provide a path to the thermal load. Shown in Figure 6, for example, is the heat pipe tactical cooler expander, interface mass, and thermal strap. Shown in Table 1 are the wall thicknesses, expander material, and supported interface masses at the cold-tip of each type of cooler.

The sizable interface masses attached to the cold finger tip can create a significant dynamic load on the expander cold finger during launch. After completing one axis of the three-axis vibration test, the radiation shield (RS) cooler did not perform correctly. Subsequent investigation of the hardware and removal of the RS cooler revealed a crack at the base of the expander that resulted in loss of helium. The expander cold finger was replaced using parts from a spare tactical cryocooler. The cooler was re-installed onto the UEP of the canister. To prevent future damage due to the launch vibrations, all three of the expanders (ISSC, radiation shield, and heat pipe cryocoolers) were fitted with constraint mechanisms designed to limit cold finger movement. Shown for each of the coolers in Table 2, with and without constraints, are the anticipated bending stresses on the cooler cold fingers during launch. The system was subsequently vibrated to proto-flight qualification levels without incident.

Table 1. Cryocooler material, wall thicknesses, and supported cold-tip masses

Cooler	Expander material	Expander wall thickness	Mass supported at cold-tip
ISSC	Stainless steel, PH 15-5	~0.152 mm (~0.006 in)	250 g (0.55 lb)
Tactical	Stainless steel, PH 15-5	~0.152 mm (~0.006 in)	164 g (0.36 lb)

Table 2. Stress summary for tactical cooler and ISSC cold cylinders

Component	Original design Pressure + Dynamic load			Revised design w/constraints Pressure + Dynamic load		
	σ_{max}	$(M.S.)_Y$	$(M.S.)_U$	σ_{max}	$(M.S.)_Y$	$(M.S.)_U$
Tactical cooler cold cylinder	137.2	- 0.24	- 0.37	55.5	1.1	0.99
ISSC cold cylinder	108.4	0.07	0.02	100.6	0.15	0.10

M.S. - Margin of Safety

$$(M.S.)_Y = \frac{\sigma_{Max}}{1.25\sigma_Y} - 1; \qquad (M.S.)_U = \frac{\sigma_{Max}}{1.25\sigma_U} - 1$$

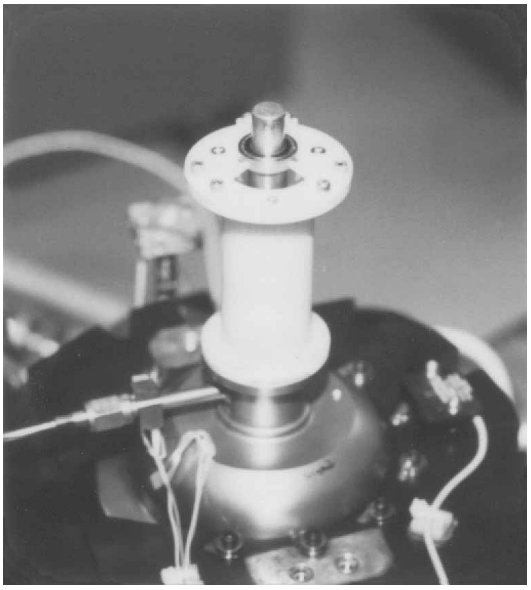

Figure 7. CSE vibration constraint for the Hughes ISSC cryocooler.

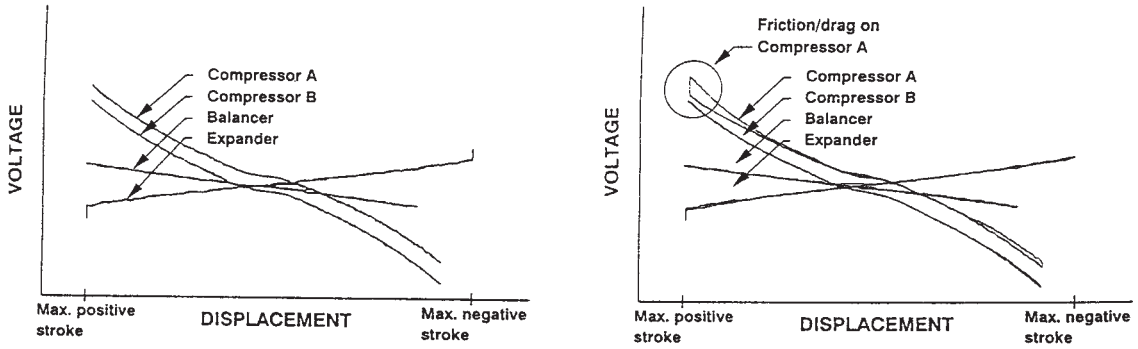

a) No contact or drag.

b) Friction at maximum positive stroke of compressor A.

Figure 8. Hysteresis plots of piston position as a function of current.

The CSE vibration constraint designs consist of two different G-10 fiberglass configurations: one for the ISSC, and one for the two tactical cryocoolers. Shown in Fig. 7 is the design for the ISSC. Note that the orientation of the fiberglass material must be considered to account for differences resulting from thermal contraction/expansion.

ISSC DIAGNOSTIC MEASUREMENT CAPABILITY

Contact resistance

The ISSC was designed with very close tolerance, non-contacting, metal-to-metal surfaces between the expander piston and its cylindrical coldfinger sidewall. Included in the design is an electrical resistance measuring circuit that indicates any momentary or prolonged contact between the expander piston and its cylinder sidewall, or its end stops. This circuit has proved essential in a number of diagnostic situations during the system integration process.

For example, during initial system checkout, the ISSC expander piston was being stroked using dc power to verify operation prior to a full system cooldown. When the piston approached to within 20% of maximum stroke, contact between the piston and cold finger wall was observed. The cause, described in detail in the next section, resulted from an excessive side load imposed on the cold finger by the thermal strap. The circuit was also useful when re-attaching the modified thermal strap to verify acceptable side loads on the cold finger. Additionally, the circuit was invaluable during system integration to verify no-contact in the final as-built state and during environmental extremes.

Hysteresis

The cooler compressor and expander designs incorporate the capability to use the position of the piston as a function of drive current to obtain a plot of the hysteresis or drag of the pistons against the cylinder side wall. Figure 8 shows two examples of hysteresis plots in which Fig. 8a represents a normal response with no friction or contact at either compressor A or B or at the expander or its balancer, and Fig. 8b represents friction or drag on compressor A at maximum positive stroke and drag starting to occur on compressor B at maximum negative stroke. This circuit was used throughout system integration to validate cooler clearances before and after component and system vibration and thermal vacuum testing. This validation is the only means to confirm that the compressor piston suspension system is operating satisfactorily following system integration and qualification tests.

HIGH-COMPLIANCE THERMAL STRAP

Design of the thermal strap connecting the cooler cold-tip to the cryogenic load must be carefully considered to achieve system performance goals. The two critical characteristics of the strap are thermal conductance and mechanical stiffness. It is desirable that the conductance be high (>0.5 W/K) due to the strong dependence of cooler efficiency on cold-tip temperature, and that the spring rate be low due to the sensitivity of the expander cold finger to mechanical side loads. It is important that these two conflicting alternatives be carefully evaluated when designing the thermal strap. The original ISSC thermal strap was designed to provide a 2.0 W/K conductance and a 5.8 lb/in spring rate in the radial direction.

When the ISSC was physically integrated onto the canister UEP and mechanically attached to the thermal strap, the expander piston was found to contact the cold finger side wall. With the thermal strap connection adjusted to a free position and the system under vacuum at room temperature, the contact reappeared when the piston traveled to 80% of maximum stroke.

Table 3. Predicted cold-tip loads for the original and modified thermal strap designs

Load	Original (lb)	Modified (lb)
Vacuum induced lid load - 0.012" cold-tip movement	0.25	0.12
Thermal contraction load - 0.020" contraction of TRP	0.43	0.20
Total anticipated Loads	0.68	0.32
Unanticipated mechanical integration load - Preload	>1.1	0.51
Total Load	>1.78	0.83
Margin @ 1.4 lb, max. acceptable load	-21%	40%

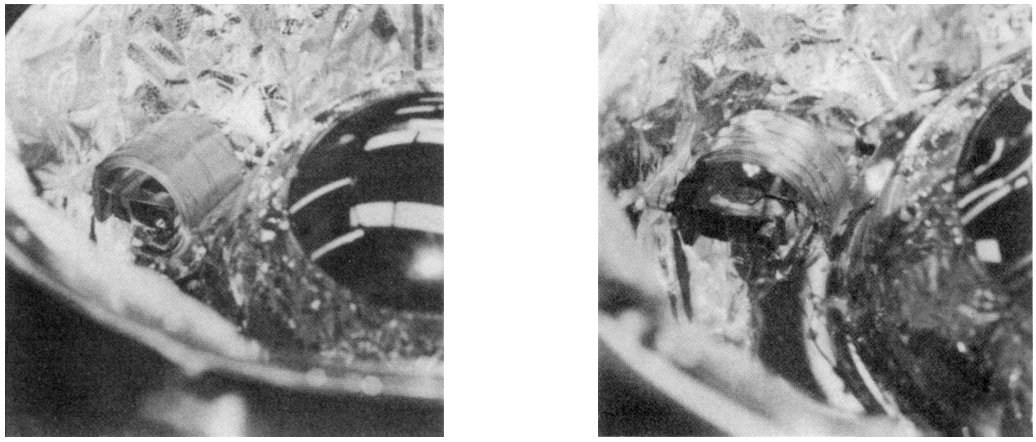

a) Original design. b) Modified design.

Figure 9. Thermal straps for the CSE ISSC.

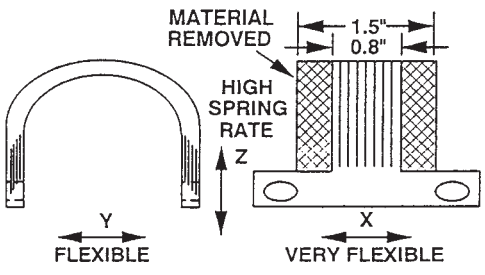

Figure 10. Modified design and references axes.

Table 4. Measured thermal strap spring rate for the original, modified, and alternate-braid designs

Axis	Original free-free (lb/in)	Modified free-free (lb/in)	Alternate-braid free-free (lb/in)
X	N/A	1.4	7.3
Y	4.0	1.6	28.5
Z	11.9	4.2	3.5

The contact remained through the TRP mass cooldown to approximately 80 K. The contact persisted with the system warmed up to room temperature, but still under vacuum. When backfilled to ambient pressure, the contacting disappeared, and then reappeared when vacuum conditions were reestablished.

The measured deflection at the center of the UEP due to vacuum was on the order of 0.007", which resulted in a calculated ISSC cold-tip movement of 0.012". The deflection due to thermal contraction of the simulated TRP mass was calculated to be on the order of 0.020".

Table 3 summarizes the predicted cold-tip loads for each of the contributive forces for both the original and modified thermal strap designs. The "unanticipated loads" are the result of unavoidable, but small alignment errors introduced when mechanically integrating the thermal strap into the system. A lesson learned is that this load must be allowed for when specifying the acceptable thermal strap spring rate. The conclusion was that the 1.78 lbs maximum side load imposed on the expander cold-tip by the original thermal strap was too large.

It was shown that due to the close tolerances within the ISSC, the total combination of forces from the thermal strap preload, thermal contraction loads and the additional force created by the canister lid deflection, was sufficient to cause contact. The force imposed by the thermal strap preload could not be directly measured, but the small amount of force resulting from the UEP deflection indicated that the original thermal strap was producing unacceptable side-load forces that resulted in contact under vacuum conditions. Although the canister vacuum would not result in lid deflection once in space (zero differential pressure), the relatively small amount of additional force created by the vacuum indicated that the thermal strap spring constant was too high.

Recalculating the required thermal conductance and verifying margin adequacy enabled consideration of reducing the cross-sectional area of the thermal strap to lower the resultant side-load force on the cold-tip. Two solutions were proposed: reducing the cross-sectional area of the existing copper foil thermal strap; and using an alternate thermal strap based on a copper braid material as the flexible element. The goal was to increase the mechanical compliance at the expense of somewhat lower thermal conductance, and thereby to reduce the side-load force imposed on the cold finger.

The original design, shown in Fig. 9a, was for a thermal resistance of 0.5 K/W and consisted of 39 layers of 0.004" x 1.5" of OFHC copper, giving a total cross-sectional area of 0.234 in^2. The layers at each end of the strap were soldered together. Additionally, the TRP interface holes were slotted to enable alignment adjustments. Figure 9b shows the design concept after modifications that resulted in a thermal resistance of 1.1 K/W and had 34 layers of 0.004" x 0.8" of OFHC copper; the resulting total cross-sectional area is 0.109 in^2.

Consideration was also given to an alternate design that involved the use of 32 compliant copper braids 1 in. in length whose design was targeted at a thermal resistance of 1 K/W. The ends of the copper braids were soldered and bolted to copper lugs. Figure 10 shows the modified design and identifies the reference axes used in Table 4. Table 4 is a comparison between the measured thermal strap spring rates for the original, modified and alternate-braid designs. It can be seen that the measured free-free spring rate of the alternate-braid concept in the Y-Axis is extremely stiff. As a result this design was not used.

The modified thermal strap was reinstalled into the CSE. There was no contact between the displacer and cold cylinder sidewall after installation of the strap, or after attaching the UEP and establishing vacuum conditions within the canister. The mechanical system was vibrated to proto-flight qualification levels and subjected to the thermal vacuum test without incident.

Table 5. Comparison of mass of coolers vs. thermal mass required for heat transfer

Item	ISSC	Rad shield cooler	Heat pipe cooler
Cooler	19 Kg (41.8 lb)	2.3 Kg (5.0 lb)	2.3 Kg (5.0 lb)
Thermal Path	23.4 Kg (51.4 lb)	5.7 Kg (12.6 lb)	7.6 Kg (16.6 lb)
TOTAL	42.4 Kg (93.2 lb)	8.0 Kg (17.6 lb)	9.8 Kg (21.6 lb)

MASS CONSIDERATIONS

Another system integration issue deals with the mass of the ISSC. To reduce the mass by approximately 15%, these second-generation cryocoolers are using integral back-to-back compressor- and integral back-to-back expander-designs. The problem is that, although the mass/volume has been reduced, consideration must be given to the thermal paths needed to conduct away the waste heat resulting from the input electrical power. For the CSE, the thermal path to the radiator, the UEP of the canister, resulted in a significant mass penalty for each of the three coolers. Shown in Table 5 is the mass of each cooler and the additional mass of the copper thermal path needed to maintain acceptable cooler operating temperatures (See Fig. 4 for the ISSC, ISSC thermal path, and the radiator).

It should be noted, however, that there are reasons for initially excluding the weight of the thermal path in a cryocooler mass calculation: 1) the required mass is dependent upon the distance from the compressor and expander to the heat rejection surface; 2) the required operating temperature (lower temperature, larger cross-sectional area) varies with the mission and radiator design; and 3) the ambient temperature to which the heat is being rejected also varies with design. The key to an optimum solution is to recognize that these factors will have to be addressed during the system integration and to include a substantial margin for mass.

CONTAMINATION/PARASITICS

One of the issues on a short mission is the effect of contaminants from the surrounding environment in the proximity of a cryogenic experiment. On a short shuttle flight (typically 7 to 10 days), there may not be adequate time for contaminants to dissipate in the vacuum environment. Since contaminants will migrate toward the coldest regions, parasitic thermal radiation loads will increase, and the test results may be negatively affected. To minimize contaminants and thermal radiation losses from the simulated TRP, an MLI-covered, anodized aluminum shield is maintained at 120 K by a tactical cooler.

Prior to installation in the canister, the mechanical system was vacuum baked to remove all contaminants. The canister was then backfilled with clean, dry nitrogen gas at approximately 3 psig. This "clean" condition will be maintained within the canister until after launch when the shuttle bay doors are opened. At this time the vent valves located on the canister lower end plate will be opened to establish vacuum conditions and the experiment timeline will be started.

SYSTEM OPERATIONS/SOFTWARE

The CSE is controlled by firmware, programmable read only memory (PROMs), in the flight electronics and is designed to automatically follow a sequence of programmed steps. The CSE software gathers and stores sensor data, controls and sequences the ISSC and tactical coolers to turn on and off, monitors and controls the operating parameters of the ISSC, and provides an operator interface for the experiment timeline.

Using Customer Ground Support Equipment (CGSE), an operator is able to monitor the progress of the experiment during the flight. Additionally, the operator can also use the CGSE to alter or modify the baseline system operations at any time during the experiment timeline.

The firmware control approach permitted the design of the electronics, typically a long-lead item, to proceed before all the requirements and the experiment operating parameters were completely defined. During system integration, corrections to the timeline and revisions to the experiment operations were able to be incorporated into the firmware without having to modify the hardware.

Controlling the system operations by software allowed for maximum flexibility in defining the system experiment, the system operational sequence, and the operating parameters of the ISSC cooler. For an experiment whose goal is to evaluate an enabling technology, this flexibility was invaluable.

ELECTRICAL INTERFACE REQUIREMENTS

Electrical interface requirements for shuttle flight experiments are relatively straightforward. The CSE used the NASA-GSFC Hitchhiker Customer Accommodations & Requirements Specifications. The focus, for tertiary Class D experiments, is on shuttle and personnel safety; fusing is provided to protect the shuttle, not the experiment. From the experiment's point of view, the source current is limited only by the fuses. The primary issue is whether or not to provide experiment safeguards and circuitry to preclude excessive current that could result in a blown fuse, and possible data loss or inability to complete the experiment.

The CSE Project chose to follow an alternative path: characterize the electrical hardware, understand the operational timeline to preclude operational sequences that could result in excessive currents, and utilize electronics hardware, software and firmware that would allow relatively easy reprogramming of the experiment timeline. Finally, CSE validated the experiment during the thermal vacuum test by following the experiment operational timeline.

Nevertheless, a key concern was the potential for the "simulated shuttle power source" to provide excessive current or voltage to sensitive circuits during electrical checkout and system integration. To preclude subjecting the flight fuses to electrical stresses induced by shorts or low-resistance paths, CSE utilized laboratory power supplies that included both current- and voltage-limiting capability. These power supplies provided protection for the flight fuses on several occasions when the CSE experienced system shutdown and reset modes during the checkout, integration and initial thermal vacuum testing.

For the pre-integration electrical checkout at GSFC, CSE has requested power supplies that include both current- and voltage-limiting capability. After integration on the cross-bay carrier with other experiments, the CSE will receive power, which will not be limited, through the Hitchhiker avionics. For subsequent pre-flight electrical checkout at KSC, power will continue to be supplied through the Hitchhiker avionics.

SAFETY

Pressurized Components vs. Pressure Vessels

For the CSE, an important safety issue was the classification of the cryocoolers and heat pipe. These components were examined by JPL using criteria from NSTS 1700.7B that addresses pressure vessels, pressurized components, and piping, tubing, and fittings. With concurrence from the Johnson Space Center, the cryocoolers and heatpipe were classified as pressurized components. As such, both cryocoolers and the heat pipe required only proof testing.

Table 6. Orbital comparison between CSE and LPE

	Elevation	Inclination	Comment
CSE	200 nm	51 °	The CSE orbit crosses the SAA and spends ~5% of its time in the SAA during a 7-day period.
LPE	135 nm	28.5 °	The LPE orbit crosses the SAA and spends ~2% of its time in the SAA during a 7-day period.

This classification resulted in a significant cost savings to the Project. It meant that the Project was exempt from providing additional items specifically for burst testing and life-cycle testing. In addition to the cost savings, there were savings associated with preparation time for the Flight Safety Reviews and the extensive traceability (paperwork) required to validate pressure vessel qualification.

Radiation Exposure Due to the Natural Space Environment - Risk Minimization

A challenge for the CSE was in procuring a control and data acquisition system that would function in the natural space environment. Candidate vendors were restricted to those having previous shuttle experience; two candidates were located, one on the West coast and one on the East coast. The West coast candidate was selected on the basis of lower cost and proximity to El Segundo, California. Additionally, since JPL had used Titan electronics for their Lambda Point Experiment (LPE), it was believed that use of this flight-proven, off-the-shelf design would result in minimum development costs for CSE.

Since the shuttle flight and orbit were not known at the time of procurement, and because the electronics were a long-lead item, the specification was released using the LPE natural space environment. When the shuttle flight and orbit were announced, it was learned that the orbit was higher and the inclination was greater than originally anticipated (see Table 6), resulting in a significantly more severe radiation environment. The CSE will be subjected to a proton flux 2 to 3 times greater than LPE, although the cosmic ray environment for both missions is similar.

The key issue was not total integrated radiation dosage, which for a 7 - 10 day shuttle mission was negligible, but rather, susceptibility of the electronics to Single Events Effects (SEE), a combination of Single Event Upset (SEU) and Single Event Latchup (SEL).

A 32K x 8 SRAM had been categorized as "high risk," being very soft to both SEU and SEL; and approximately 40 parts had been identified for which no SEE susceptibility data were available at JPL. Replacing these parts within the CSE control and data acquisition system would require a major redesign that was unacceptable in terms of both cost and schedule. Substitution of equivalent radiation-hardened parts was not practical based upon lack of compatibility, lack of availability, and relatively high cost.

Testing to validate acceptable performance in the natural space environment was too costly, and not consistent with the delivery schedule. Additionally, measured performance of the parts would not resolve the issue, only provide more detailed knowledge about the parts.

An assessment team, consisting of circuit designers/system engineers from the CSE Project, and electronics parts reliability and natural space environment (radiation) specialists from JPL, was tasked with resolving the problem. Their approach was to: 1) determine the shuttle exposure profile to the South Atlantic Anomaly (SAA), 2) re-estimate the radiation environment and CSE shielding impacts, 3) develop a better understanding of the questionable parts, associated manufacturers and circuit technology, 4) reduce the parts list by discarding non-

susceptible parts and assess risk of SEU and SEL for those remaining, 5) identify suspect part flight histories and radiation data, 6) identify and assess impact of hardware and software modifications for enhanced immunity, problem determination and recovery, and 7) establish and compare the radiation environment between LPE and CSE.

The CSE shuttle exposure profile consists of SAA exposure during approximately 5% of the mission, usually in blocks of 9 consecutive orbits, with cosmic rays accounting for another 5%. The environment is severe enough (5 - 100 MeV) to cause SEUs in non-qualified parts (parts having a threshold of 0.4 MeV are expected to experience 0.1 upsets per 24-hours of exposure). Shielding was found to provide little improvement.

Electronic parts pare down resulted in eliminating a number of parts and identifying 21 remaining parts with unknown susceptibility. Of these 21 remaining parts, 10 were eliminated by the CSE Project due to circuit function (resets or loss of which is insignificant). Further review of SEE circuit operational impact (hardware/flight software modifications) indicated that the use of bus architecture precluded meaningful assessment, and that no cost-effective modifications were identified.

The LPE exposure to radiation was less severe. LPE hardware flew at 135 nautical miles (nm) versus 200 nm expected for CSE. At this altitude, the radiation environment intensity (proton flux) doubles with each 100 nm increase in altitude. LPE experienced SEUs.

The assessment team indicated that 11 identified parts may experience SEUs (<0.1 SEU per 24 hours of exposure, total mission exposure determined to be 7 hours, 42 minutes). It is costly and late in the program to retrofit a change (Class D experiment assumes manageable risk). To minimize risks associated with the SAA, the assessment team recommended modifications to ground support procedures to: 1) allow operator intervention and custom commanding, 2) utilize power standby or power off modes during SSA exposure (30-minutes down time maximum), and 3) target benign experiment operations during SAA exposure (critical data gathering to occur during non-exposed orbits).

The lesson learned is that when a project cannot afford radiation-hard electronics, it is necessary to understand the natural space environment based upon the shuttle flight inclination and orbit as early as possible to allow for a complete assessment of the single event effects upon the electronic parts.

Reliability/Quality Assurance - In-Process Checks/Inspection Points

A challenge with any new design is the establishment of meaningful and timely in-process inspections points, as well as performance and verification checks. Some of the checks that were performed on the CSE included mechanical inspections and fit checks of the hardware during fabrication. These checks minimized the mechanical integration problems associated with a first-time build. Other checks that were performed included the verification of sensors, continuity checks on the system cabling, and electronic checkouts. Additionally, the software was developed and checked out using an emulator prior to the final design being burned into the flight μprocessor.

In some cases additional checks and inspection points were established after problems had been discovered. One example occurred during the mechanical integration of the thermal strap between the ISSC expander cold-tip and the simulated TRP, previously discussed. The piston/cylinder contact signal was monitored to validate that the thermal strap was reintegrated in a position with no side loads.

Another example occurred when the vibration constraints were added to the cryocooler expanders after the RS tactical cooler expander failed during the vibration test. In this case, the

tactical cooler input power was monitored for any changes during the reassembly process. An increase in input power was indicative that a side load configuration existed, and the constraint needed adjustment.

To minimize problems associated with the CSE mechanical integration, a full-scale mockup of the experiment canister and the mechanical components was fabricated. A non-flight UEP was used as a template for fit checks of the flight structural members, cryocooler heat sinks and mechanical component clearances during hardware fabrication. An additional benefit of the full-scale mockup was in being able to check the electrical cable routes and lengths prior to installation of the connectors.

The lesson learned was that a well-thought out inspection and in-process verification plan, coupled with a full-scale mockup, saved valuable amounts of time in a fast-track program by anticipating problem areas, identifying critical assemblies and processes, and verifying that the assembly/process was correct before proceeding with the final assembly. Additionally, when a problem did occur, revisiting the inspection timeline and revising inspection points were included as a part of the corrective action process to preclude the problem from reappearing.

SUMMARY

The NASA IN-STEP CSE has provided an opportunity to identify and resolve a number of cryogenic system interface integration issues that normally would not be addressed until a cryogenic cooling system was selected for integration into a multi-year space mission. It is hoped that the challenges and problems encountered in the system integration of these enabling technologies will provide insight to system designers of imaging-instrument systems incorporating long-life cryogenic cooling systems.

ACKNOWLEDGEMENT

The work described in this paper was carried out by Hughes Aircraft Company, Electro Optical Systems, under a contract with the Jet Propulsion Laboratory, California Institute of Technology, under a contract with the National Aeronautics and Space Administration.

Particular credit is due Bradford Wolf, Phil Mayner, and Dave Gilman of Hughes, whose dedication and diligence in identifying and resolving the issues and challenges is deeply appreciated.